

3 The Solar X-Ray Flare
of 7 July 1966* 6

by

6 J. A. Van Allen 9

2 Department of Physics and Astronomy
| University of Iowa
Iowa City, Iowa, U.S.A.

9 July 1967 1004

25A
* Supported in part by National Aeronautics and Space Administration Contract NAS5-9076 and by Office of Naval Research Contract Nonr-1509(06).

ABSTRACT

By means of a mica window Geiger-Mueller tube on earth satellite Explorer 33, a major solar x-ray flare was observed with 81.8 sec time resolution on 7 July 1966. The flare had its onset at 00:23, its maximum intensity at 00:42, and a total duration of about 200 minutes. The maximum energy flux was 3×10^{-2} ergs/cm² sec and the time integrated flux was 97 ergs/cm² ($2 < \lambda < 12^\circ \text{ A}$). Assuming equal intensity over 2π steradians at the sun, the total emission in this wave length band was 1.4×10^{29} ergs and the maximum surface luminosity of the sun was 2.9×10^6 ergs/cm² sec or 4.5×10^{-5} of the whole radiant luminosity of the average solar surface. Charged particles began to arrive at the satellite at 00:58, or 35 minutes after the first detection of the x-ray enhancement, and remained in the interplanetary system for at least ten days thereafter. The intensity-time curve of the soft x-rays is compared with those of 2700 MHz solar radio noise flux and of ionospheric absorption at 22 MHz as observed at Penticton.

I. OBSERVATIONAL TECHNIQUE

The Satellite

A major solar x-ray flare was observed on 7 July 1966 by University of Iowa equipment on the satellite Explorer 33 of the Goddard Space Flight Center/National Aeronautics and Space Administration. This satellite was launched at 16:02 U.T. on 1 July 1966 into an eccentric orbit about the earth with its initial apogee at a geocentric radial distance of about 440,000 km. The satellite is "spin-stabilized", i.e., it is set spinning about its axis of maximum moment-of-inertia during the launching operation. Ideally, the spin period is constant thereafter as are the celestial coordinates of the spin axis. In the present case, there are weak torques, due primarily to solar light pressure, which produce slow changes in all of these parameters. Early on 7 July 1966, the spin period was 2.286 seconds and the right ascension and declination of the spin axis were 225.1° and -21.2° , respectively. The right ascension and declination of the sun were 105.8° and $+22.6^\circ$. Hence, the angle α between the spin axis and the satellite-sun vector was

$$\alpha = 124.1^\circ.$$

Detector

Of the system of four University of Iowa detectors [Van Allen and Ness, 1967] the following one is pertinent to the present report:

GM 1: An EON 6213, mica window Geiger-Mueller tube having a 1.7 mg/cm^2 thickness window and a fan-shaped collimator whose central axis is orthogonal to the spin axis of the satellite. As measured experimentally with a soft x-ray beam (electron energy 2.0 kV) in vacuo, the full angle of the collimator is 45° in the equatorial plane of the satellite and 79° in the meridian plane.

The GM tube is a self-quenching one filled to a total nominal pressure of 429 mm Hg (at 0° C) with neon (410 mm), argon (7 mm), and chlorine (12 mm) [N. Anton, private communication]. The effective volume of the tube for soft x-rays is a cylinder 0.7 cm in length and 0.24 cm in diameter. The x-ray efficiency of the tube has been determined by two methods.

(a) By calculation [cf. Van Allen et al., 1965 for the method as applied to a different batch of tubes having thinner windows and a shorter gas path].

(b) By experimental comparison with a longer path-length, beryllium window, argon filled EON 6312 tube whose efficiency can be calculated with better accuracy. In this experimental work [C. D. Wende] a crystal spectrometer was used. The two tubes under comparison were

exposed in turn to the collimated, dispersed beam from a small x-ray tube in vacuo. The absolute photon efficiency $\epsilon(\lambda)$ as determined in this way is shown in Figure 1. The K absorption edges of the principal constituents of mica--nominally $\text{H}_2\text{K Al}_3 (\text{Si O}_4)_3$ --appear clearly. The smooth curve is one of the form and absolute value resulting from method (a) after choosing a window thickness and a gas path for a best fit to the experimental data. The chosen values of the two latter parameters lie within the some 15% uncertainty in their determination by other methods. The experimental data depart significantly from the smooth (calculated) curve only in the wavelength region $\lambda < 2.6 \text{ \AA}$. The departure here may be due to L absorption edges of minor constituents of the fill gas, I and Xe being conceivable possibilities. The portion of the curve $\lambda < 2.6 \text{ \AA}$ is of little importance in the present work and the smooth curve has been adopted throughout. This curve is believed to represent the absolute photon efficiency of GM tubes of the batch used in Explorer 33 with an uncertainty not greater than 30% for $\lambda > 2.6 \text{ \AA}$.

These tubes were exposed in the laboratory to the ultra-violet beam of a hydrogen arc delivering the equivalent intensity in the 1000 \AA range of several times that of the solar Lyman-alpha line. There was no detectable response [L. A. Frank]. On the basis of this and other evidence it is assumed henceforth that the mica-window tubes are completely insensitive to solar ultra-

violet as well as to the visible (the latter being easily demonstrated).

Based on the smooth curve of Figure 1, the curve of Figure 2 shows the absolute energy flux $F(\lambda)$ in ergs/cm² sec of monochromatic radiation of wavelength λ required to produce one count/sec. This curve is for a beam parallel to the axis of the tube (i.e., perpendicular to the face of the window). For rough purposes, it may be approximated by a constant value 1.8×10^{-6} ergs/cm² count for $2 < \lambda < 12 \text{ \AA}$ and infinity elsewhere.

For a given spectrum the ratio of energy flux to counting rate can be calculated numerically using the curve of Figure 1. Thus,

$$\frac{F(0 - \lambda)}{R} = \frac{\int_0^{\lambda} F(\lambda') d\lambda'}{a \int_0^{\infty} \epsilon(\lambda') n(\lambda') d\lambda'}$$

where $F(0 - \lambda)$ is the energy flux in the wavelength range 0 to λ for a spectrum which in its entirety produces a counting rate R ; a is the effective area of the aperture of the GM tube (0.045 cm^2); $F(\lambda')$ and $n(\lambda')$ are the differential energy flux and differential photon number flux (both per unit wavelength), respectively; and

$$F(\lambda') = \frac{hc}{\lambda'} n(\lambda') .$$

Illustrative values of $F(0 - \lambda)/R$ have been calculated for several cases:

Case A

$$\begin{aligned} n(\lambda') &= 1, & \text{for } 1 \text{ A}^\circ < \lambda' < \lambda \\ &= 0, & \text{for } \lambda' > \lambda \end{aligned}$$

Case B

$$\begin{aligned} F(\lambda') &= 1, & \text{for } 0 < \lambda' < \lambda \\ &= 0, & \text{for } \lambda' > \lambda \end{aligned}$$

Case C

$F(\lambda')$ and $n(\lambda')$ are Planck black body functions for $T = 1 \times 10^6$, 2×10^6 , 5×10^6 , and 1×10^7 deg Kelvin [Allen, 1963].

The results are summarized in Table 1 from which it is seen that

$$\frac{F(2 - 12 \text{ A}^\circ)}{R} = 1.8 \times 10^{-6} \frac{\text{ergs}}{\text{cm}^2 \text{ count}}$$

is a good approximation for any observed form of solar x-ray spectrum, including one having a distribution of emission lines superimposed on a continuum [Culhane et al., 1964] [Friedman, 1964] [Mandel'stam, 1965] [Walker and Ruge, 1967]. This value is adopted for subsequent calculations of absolute energy fluxes.

Table 1

Ratio of Energy Flux $F(0-\lambda)$ Integrated
over Wavelength Range 0 to λ A° to
Counting Rate R of Geiger Tubes on Explorer 33
for Six Exemplary Spectra
(units of $\frac{F(0-\lambda)}{R}$ are microergs/cm² count)

λ		Case A	Case B	Case C			°K
				1×10^6	2×10^6	5×10^6	1×10^7
1	A°	-	-	-	-	-	0.0006
2		31.	59.	-	-	0.006	0.138
3		9.7	11.5	-	-	0.026	0.562
4		5.2	5.0	-	-	0.142	0.99
5		3.5	3.0	-	0.004	0.34	1.31
6		3.1	2.6	-	0.029	0.58	1.52
7		3.0	2.5	-	0.106	0.81	1.66
8		2.8	2.3	0.023	0.27	1.02	1.76
9		2.6	2.0	0.094	0.54	1.20	1.83
10		2.5	1.9	0.35	0.91	1.34	1.88
11		2.5	1.9	1.05	1.38	1.46	1.92
12		2.5	2.1	2.3	1.90	1.56	1.95
13		2.6	2.2	4.9	2.48	1.64	1.97
14		2.7	2.4	9.1	3.09	1.71	1.98
15		2.7	2.6	14.3	3.70	1.77	2.00
20		3.0	3.4	78.2	6.5	1.94	2.03
30		3.4	5.2	321.	10.0	2.05	2.05
50		4.0	8.6	742.	12.4	2.10	2.06
∞		-	-	1170.	13.7	2.12	2.06

Sector Generator

An electronic sector-generator [D. C. Enemark] is triggered by a "see-sun" pulse from a narrow angle photo-electric sensor. This generator gates pulses from GM 1 into four separate storage registers, one register for each quadrant of rotation and adjusts its rate of sectoring automatically to maintain this performance as the spin period changes (slowly) with time. This process continues for 25.57 seconds and the contents of each register are read out over the telemetry system each 81.808 seconds (one "sequence"). Thus, the storage time for each quadrant is 6.39 seconds (distributed over a 25.57 second period) and one such reading is obtained each 81.808 seconds (the resolution time). The timing of the telemetry system is independent of the spin period. On rare occasions a fortuitous, and temporary, synchronization between the spin period can produce a persistent inequality in the sampling times of the four, nominally equal sectors. On 1 July there were 11.19 rotations per 25.57 seconds. Thus, during any one sequence, a given quadrant may contain as much as 8% more sampling time than the other three. Over a series of sequences this effect is averaged among the four quadrants and is trivial for the present purpose, as is the inherent inaccuracy of the sector generator.

Sector Response of Detector

The spin axis of the satellite has a solar ecliptic latitude -3.9° . Hence the four quadrants of the GM 1 detector respond as follows (Figure 3).

	<u>Omnidirectionally</u>		<u>Directionally (Approx.)</u>
Sector I	Penetrating Particles		Particles from direction of anti-sun
Sector II	"	"	Particles from north ecliptic pole
Sector III	"	"	Solar x-rays and particles from direction of sun
Sector IV	"	"	Particles from south ecliptic pole

On 7 July 1966, the satellite was on the sunward side of the magnetospheric shock wave at a geocentric distance of 68 earth radii. Hence Sectors I, II, and IV respond only to galactic and solar cosmic ray particles, whereas Sector III responds to such particles plus solar x-rays. Hence the quantity

$$GLX = R_{III} - (R_I + R_{II} + R_{IV})/3$$

where R_i is the counting rate of the i^{th} sector, is the net counting rate in Sector III due to solar x-rays. It is here assumed that the average rate of Sectors I, II, and IV is equal to the non-x-ray counting rate of Sector III. This is not true for solar cosmic ray beams on some occasions. However, reasonably valid

assessment of the error thus involved can be made by examining the relative value of R_I , R_{II} , and R_{IV} as well as those of two other similar GM tubes (GM 2 and GM 3), which receive particles from other directions [Van Allen and Ness, 1967].

Geometric Obliquity Factor

In the preceding analysis of the absolute x-ray efficiency of GM 1, it has been supposed that the beam of x-rays is incident parallel to the axis of the tube. Under flight conditions the collimator sweeps through the solar beam as the satellite spins, producing a counting rate peak (not observed directly) near the center of Sector III's sampling time during each rotation. Hence the average counting rate of Sector III, which is the observed quantity, must be multiplied by an appropriate factor to obtain the counting rate which would have occurred if the axis of the collimator of GM 1 had been constantly along the satellite-sun line. This geometric obliquity factor is a function only of the angle α between the spin axis and the satellite-sun line. It is designated $f(\alpha)$.

Values of $f(\alpha)$ have been determined experimentally using a heterochromatic, collimated beam from a small x-ray generator operated at 2.0 kilovolts ($\lambda \geq 6.2 \text{ \AA}$). Some sample values of $f(\alpha)$ from a comprehensive set of angular experiments [Sister J. Gibson] are tabulated in Table 2. Note that $f(\alpha) = f(180 - \alpha)$.

Specifically $f(124.1^\circ) = 81$.

Table 2

Geometric Obliquity Factor

α	$f(\alpha)$
90 (90)	4.85
80 (100)	7.41
70 (110)	15.6
60 (120)	40.
55 (125)	96.

Dynamic Range and Sensitivity of Detector

The apparent counting rate r of GM 1 is an accurately linear function of the "true" counting rate R (as would be observed by an idealized system with zero dead time) for $0 < R < 3 \times 10^3$ counts/sec and is a monotonically rising and well measured function of R up to $R = 1 \times 10^5$ counts/sec. (Values of R as great as 10^6 counts/sec can be estimated using the falling branch of the r vs R curve.) These considerations and the appropriate value of $f(\alpha)$ determine the upper portion of the dynamic range.

The lower limit of the dynamic range of the system at $\alpha = 90^\circ$ (the most sensitive case) is found as follows in the presence of galactic cosmic rays only. The "background" rate is 0.6 counts/sec or 3.8 counts per 6.39 sec sample per sector (one sequence). During ten sequences (13.6 minutes) the expected number of background counts per sector is 38 ± 6 . Hence an x-ray contribution to GLX of ~ 20 counts during such a period, or 0.3 counts/sec is clearly detectable. This corresponds to 3×10^{-6} ergs/cm² sec ($2 < \lambda < 12 \text{ A}^\circ$). For 100 sequences, a flux of 1×10^{-6} ergs/cm² sec is clearly detectable, etc. At other values of α , the level of detectability is increased by a factor $f(\alpha)/f(90^\circ)$ (Table 2).

The GM detector measures, of course, the x-ray emission from the whole visible hemisphere of the sun and has only crude spectral resolution as described in detail above.

But its high sensitivity and large dynamic range ($\sim 10^5$ in favorable cases) are noteworthy.

II. OBSERVATIONS OF THE 7 JULY 1966 FLARE

In Figure 4 are plotted, in full available detail, the raw responses of GM 1--Sectors I and III as a function of time for the period 21:37 on 6 July to 04:25 U.T. on 7 July 1966. A similar plot for GM 1--Sectors II and IV is given in Figure 5.

From Figures 4 and 5 it is seen that

- (a) There were two minor x-ray flares, each of ~ 10 minutes duration, late on 6 July with maxima at 21:53 and 22:29, respectively.
- (b) On 7 July, a major x-ray flare had its observed onset at 00:23 and its maximum intensity at 00:42 (Sector III). At 00:58 ± 3 (35 minutes after the onset of the x-ray event) particles began arriving at the satellite and their intensity rose to an approximately constant value by $\sim 04:00$ (Sector I).
- (c) A small "ghost" response during the maximum intensity of the x-ray flare was detected by Sectors II and IV, but not by I. This ghost response ($\sim 2\%$ of that on III) on Sectors II and IV which are rotational adjacent to III has been observed in other, but not all, intense events. It is not anticipated from the laboratory calibrations using x-rays with $\lambda > 6 \text{ \AA}$ and is believed to be due to harder x-rays scattered off the inner walls of the collimator and, perhaps, penetrating the lips of the collimator in such a way as to violate the nominal angular limits of

the collimator. An attempt is being made to confirm this belief by laboratory test. Meanwhile, based partly on internal evidence and partly on private communications from other investigators who are observing hard x-rays ($\lambda \lesssim 0.2 \text{ \AA}$) from the sun the magnitude of the ghost response on Sectors II and IV is regarded as an indicator of the intensity of hard x-rays. (The ghost effect is not seen in GM 2 and GM 3 and hence cannot be due to side wall penetration of the shield of GM 1.)

In Figure 6 is shown the net solar x-ray counting rate of Sector III. The solid points were derived from the $R_{\text{III}} - R_{\text{I}}$ difference and the x's from the GlX formula quoted above. The III-I difference was preferred before 02:00 on 7 July because of effect (c) noted above, whereas the GlX formula gives somewhat better statistical accuracy and a more valid subtraction of particle effects, at later times. The broad peaks at 02:17 and 02:57 may be spurious in the sense that they may be due to inadequate subtraction of particles whose anisotropy favored Sector III. For the same reason the portion of the curve beyond 02:17 is of less validity in representing the history of the x-ray intensity than the earlier portion.

There is a small but significant pause in the increase of intensity at 00:25 and a more prominent one at 00:35. Thus

the increase of intensity to its maximum value is a composite of three phases:

00:23 to 00:25

00:26 to 00:35

00:35 to 00:42

The increase during the second phase, from 00:26 to 00:35, is well represented by $1 - \exp(-\Delta t/3.8 \text{ min})$, where $\Delta t = 0$ at 00:26 and the asymptotic value of the counting rate is taken to be 150 counts/sec. The decline of intensity (ambient pre-flare intensity subtracted) from 00:42 to 02:00 is accurately exponential in form with an e-folding time of 36 minutes. The further decline after 02:17 (no data between 02:00 and 02:17) is complex and/or less trustworthy (see above remark) but has a similar e-folding time.

The ratio of maximum x-ray intensity to the pre-flare ambient value is 28, in the pass band of the detector, $2 < \lambda < 12 \text{ \AA}$, in the sense discussed in a previous section.

On the right hand side of Figure 6 is an approximate scale of absolute energy flux taking $F(2 - 12 \text{ \AA})/R = 1.8 \times 10^{-6}$ ergs/cm² count and $f(\alpha) = 81$. The maximum value of the flux is 3×10^{-2} and the ambient quiescent value 1.1×10^{-3} ergs/cm² sec. The time integral

$$\int_{00:23}^{03:45} F' dt = 97 \text{ ergs/cm}^2 \quad \text{at} \quad 1 \text{ A.U.},$$

where F' is the difference between the total energy flux and the pre-flare or "quiet sun" flux.

Assuming equal flux over 2π steradians at the sun, the total emission was 1.4×10^{29} ergs ($2 < \lambda < 12 \text{ \AA}$).

As shown previously (Figures 4 and 5) particles began arriving at Explorer 33 near the earth at 35 minutes after the onset of the x-rays or 16 minutes after the x-ray intensity maximum, these latter two events at 00:15 U.T. and 00:34 U.T. (time at the sun). Hence the propagation time for the particles was probably between 43 and 24 minutes, corresponding to $\beta = v/c = 0.19$ and 0.35 , for rectilinear propagation. The corresponding (minimum) values of kinetic energy are $E_e = 9.5$ and 35 keV , $E_p = 11$ and 65 MeV , $E_\alpha = 45$ and 260 MeV . The presence of low energy protons and alpha particles from this flare was detected with Explorer 33 until 16 July, after which additional particles from another flare were added to the interplanetary system [Krimigis, Van Allen, and Armstrong, 1967]. A full analysis of the particle event will be published elsewhere.

III. OTHER RELEVANT INFORMATION

The foregoing discussion has been based exclusively on observations with Explorer 33.

The relationships of the x-ray flare to other phenomena will now be sketched in a preliminary way with the help of solar and terrestrial data from other observers [Solar-Geophysical Data, Environmental Science Services Administration, Boulder, Colorado, 1966] [Hakura, 1967].

On 6-7 July 1966 there were reported three H α optical flares which appear to be relevant to the x-ray intensity-time history in Figure 6 herein. These are listed in Table 3.

The first two correspond to the x-ray flares whose maxima were at 21:53 and 22:29 U.T. on 6 July. The third and much more intense flare corresponds in accurate time detail to the major x-ray flare which is the principal subject of the present paper. Thus an intimate association between H α and soft x-ray emission is apparent, and there is no reasonable doubt as to the positional origin of the x-ray emission.

Table 3

Relevant Optical Flares on 6-7 July 1966
 [ESSA, CRPL-FB-267 of November 1966]

<u>Observed U.T.</u>		<u>Max. Phase</u>	<u>Lat.</u>	<u>Meridian Distance</u>	<u>Importance</u>	<u>McMath Plage Region</u>
<u>Start</u>	<u>End</u>					
21:51	22:15	21:53	N36	W48	-B	8362
22:22	22:42D	22:29	N36	W48	-N	8362
00:26	01:27D	00:43	N34	W48	2B	8362

The "corrected" area of the optical flare is reported as about 10 heliographic square degrees, or a physical area of $1.5 \times 10^{19} \text{ cm}^2$.

The maximum (at 00:42) directional intensity of soft x-ray emission by the flare was $6.8 \times 10^{24} \text{ ergs/sec steradian}$. Hence, the surface brightness of the nominal flare area was $4.5 \times 10^5 \text{ ergs/cm}^2 \text{ sec steradian}$. Over an assumed 2π steradians the maximum soft x-ray ($2 < \lambda < 12 \text{ \AA}$) luminosity of the flare area was, therefore,

$$2.9 \times 10^6 \text{ ergs/cm}^2 \text{ sec},$$

or 4.5×10^{-5} of the whole radiant luminosity of the average solar surface.

In addition to enhanced x-ray and optical emission and noteworthy acceleration and emission of energetic particles [Krimigis, Van Allen, and Armstrong, 1967], there was a wide variety of enhanced radio emission [see compilation of Hakura, 1967]. A sample of such observations is the recording of solar radio noise at 2700 MHz by the Dominion Radio Astrophysical Observatory at Penticton, B. C. It is reproduced in Figure 7 from ESSA/CRPL-FB-264 of August 1966. There is a general resemblance between this complex curve and the x-ray flux curve but the two are quite different in detail. The physical association between the two phenomena appears to be of a general rather than an intimate nature.

The most relevant terrestrial observation is that of the ionospheric (D-layer) absorption of cosmic radio noise [Friedman, 1964]. Such a curve, also from Penticton, at 22 MHz is reproduced from Hakura's paper [1967] in Figure 7. The detailed resemblance to the soft x-ray curve (including the pause in the leading side at 00:35) is striking.

No further interpretation is undertaken herein but it is hoped that the detailed, quantitative record of the 7 July 1966 x-ray flare will be of value to other workers in the fields of solar and ionospheric physics.

REFERENCES

- Allen, C. W., Astrophysical Quantities, Athlone Press, London 1963.
- Culhane, J. L., A. P. Willmore, K. A. Pounds, and P. W. Sanford, "Variability of the Solar X-Ray Spectrum below 15 A°", pp. 741-758 of Space Research IV, North-Holland Publishing Co., Amsterdam (ed. by P. Muller), 1964.
- Friedman, H., "Ionospheric Constitution and Solar Control", pp. 197-241 of Research in Geophysics, Vol. I, M.I.T. Press, Cambridge, Mass. (ed. by H. Odishaw), 1964.
- Hakura, Y., "The Polar Cap Absorption of July 7-10, 1966", Goddard Space Flight Center Report X-641-67-116 of March 1967.
- Krimigis, S. M., J. A. Van Allen, and T. P. Armstrong, "Simultaneous Observations of Solar Protons Inside and Outside the Magnetosphere", Phys. Rev. Letters, 18, 1204-1207, 1967.
- Mandel'stam, S. L., "X-Ray Emission of the Sun", Space Science Reviews, IV, 587-665, 1965.
- Van Allen, J. A., L. A. Frank, B. Maehlum, and L. W. Acton, "Solar X-Ray Observations by Injun I", J. Geophys. Res., 70, 1639-1645, 1965.
- Van Allen, J. A., and N. F. Ness, "Observed Particle Effects of an Interplanetary Shock Wave on July 8, 1966", J. Geophys. Res., 72, 935-942, 1967.

Walker, A. B. C., Jr., and H. R. Rugge, "Variation in the Solar X-Ray Line Spectrum Below 25 A°", Paper No. 11.07, 124th Meeting of the American Astronomical Society, June 1967.

White, W. A., "Solar X-Rays: Slow Variations and Transient Effects", pp. 771-779 of Space Research IV, North-Holland Publishing Co., Amsterdam (ed. by P. Muller), 1964.

FIGURE CAPTIONS

Figure 1. Absolute photon efficiency of GM 1 (EON 6213 Geiger-Mueller tube) for a soft x-ray beam parallel to the axis of the tube. $\epsilon(\lambda)$ is the number of counts per photon of wavelength λ incident within the effective diameter of the tube (0.24 mm).

Figure 2. Absolute energy flux efficiency of GM 1.

Figure 3. University of Iowa sectoring scheme on Explorer 33.

The axis of the collimator of GM 1 is 130° counterclockwise from the axis of the "see-sun" sensor which initiates the gating of counts into four separate registers, each of which receives counts during successive quadrants of rotation as shown. The spin axis lies approximately in the ecliptic plane. The angle between the spin axis and the satellite-sun line was 124.1° on 7 July 1966.

Figure 4. Raw counting rate data from Sectors I and III of GM 1.

Figure 5. Raw counting rate data from Sectors II and IV of GM 1.

Figure 6. Time dependence of soft x-ray ($2 < \lambda < 12 \text{ \AA}$) intensity.

Absolute energy flux is given by the scale on the right.

The circles are derived from the $(R_{\text{III}} - R_{\text{I}})$ counting rate difference and the X's from the formula

$$RLX = R_{\text{III}} - (R_{\text{I}} + R_{\text{II}} + R_{\text{IV}})/3.$$

Figure 7. Comparison of the intensity-time curve for soft solar x-rays with those for solar radio noise at 2700 MHz and ionospheric absorption of cosmic radio noise at 22 MHz [ESSA, 1966 and Hakura, 1967]. All three curves are semi-logarithmic with a factor of ten between major divisions on the vertical scale.

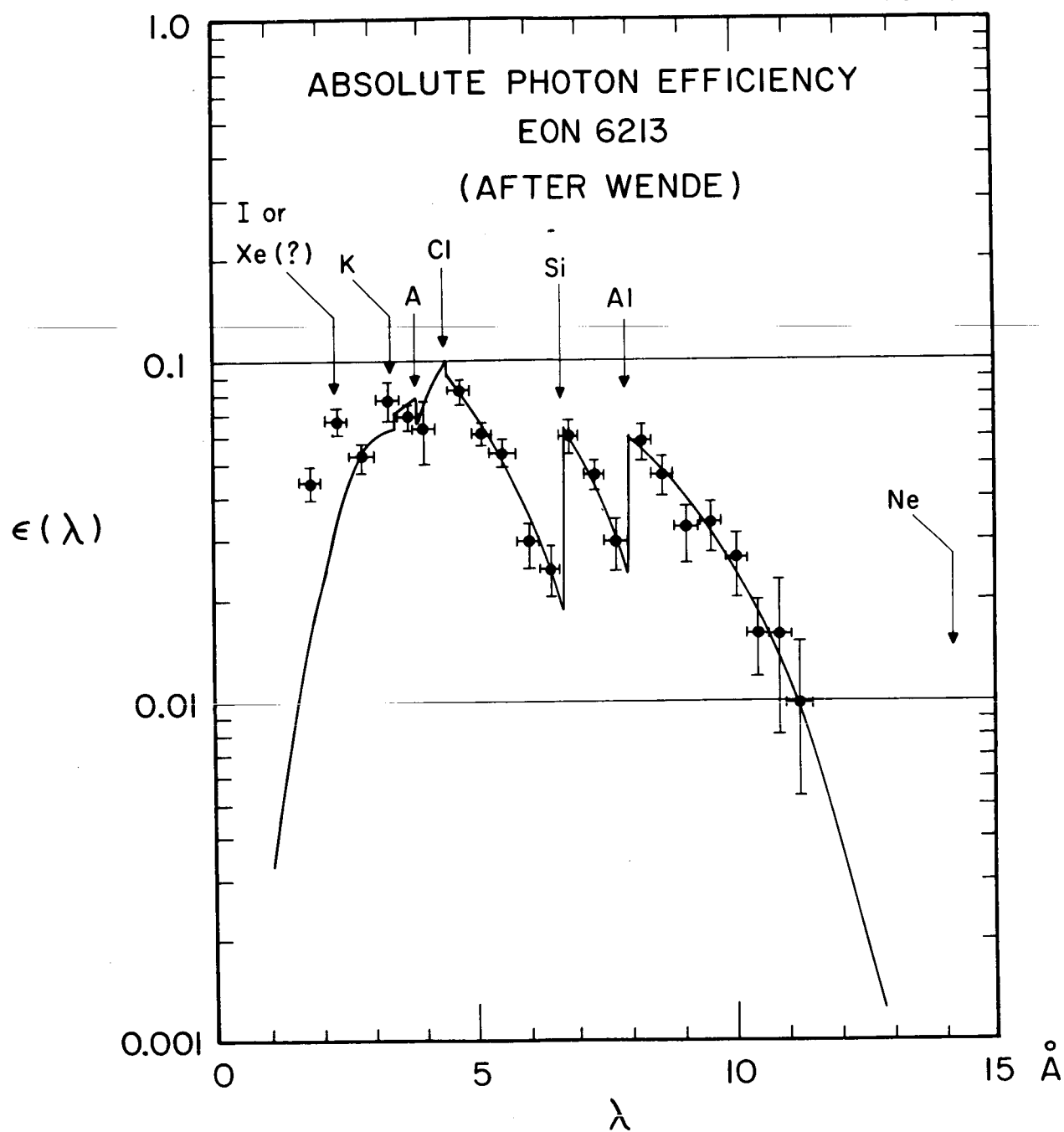


Figure 1

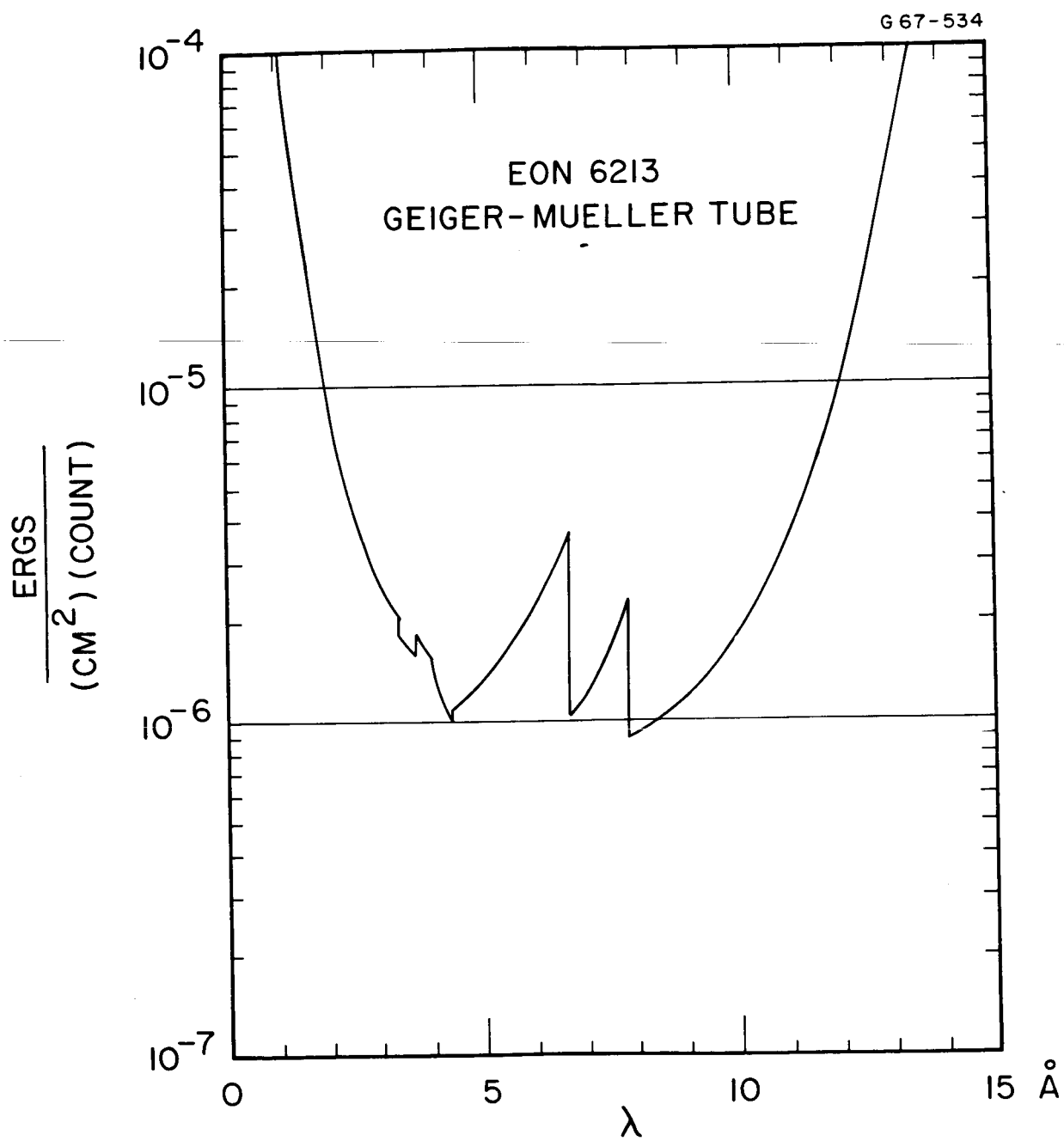


Figure 2

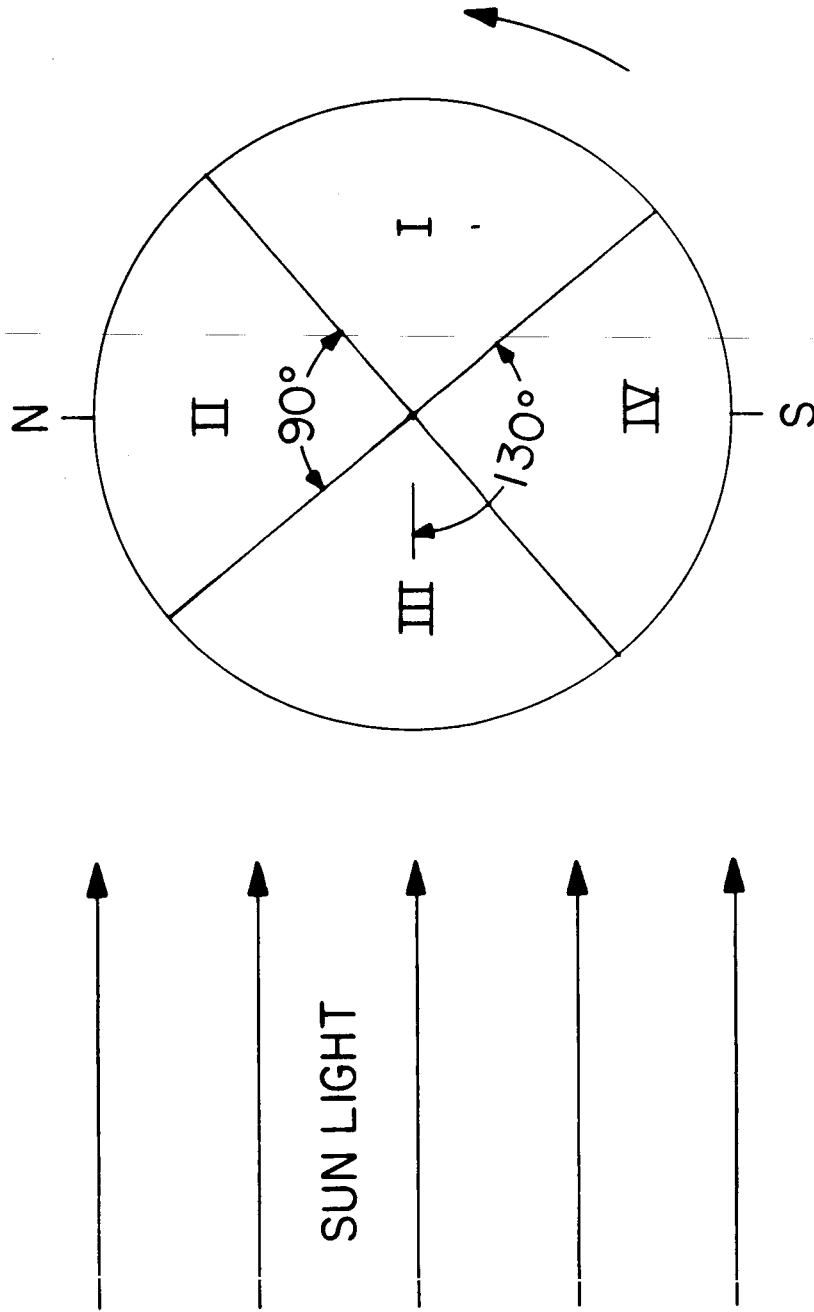


Figure 3

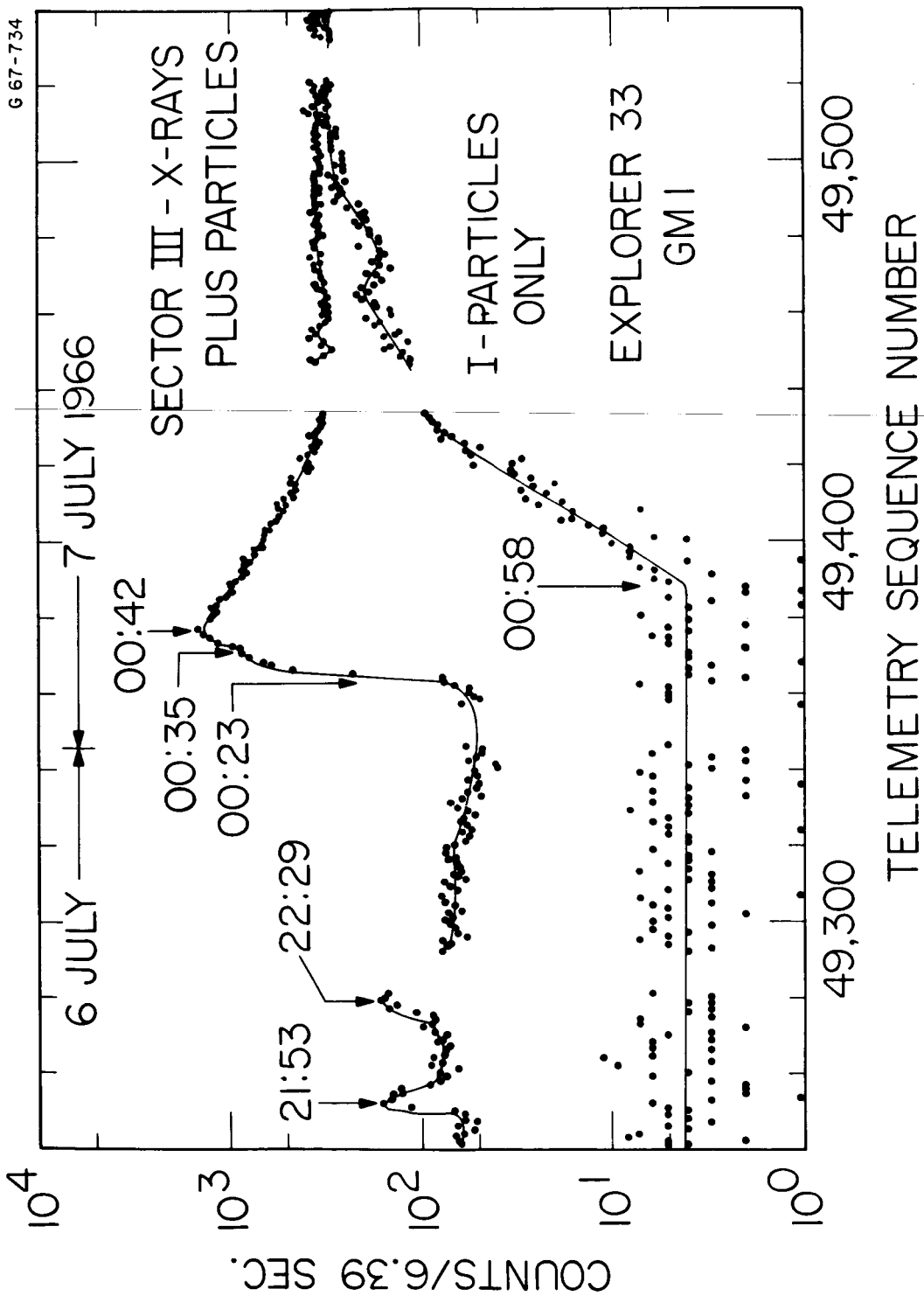


Figure 4

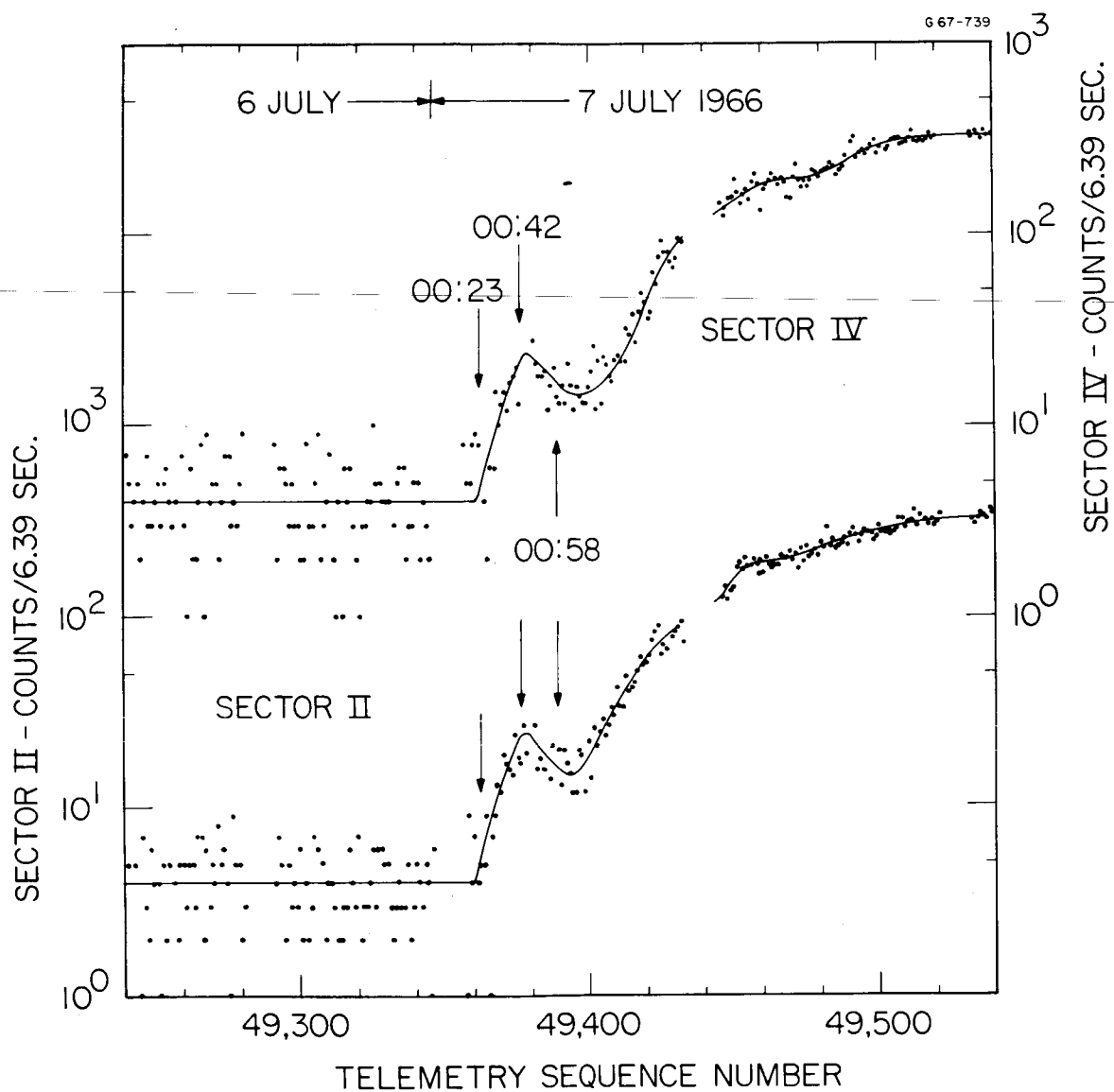


Figure 5

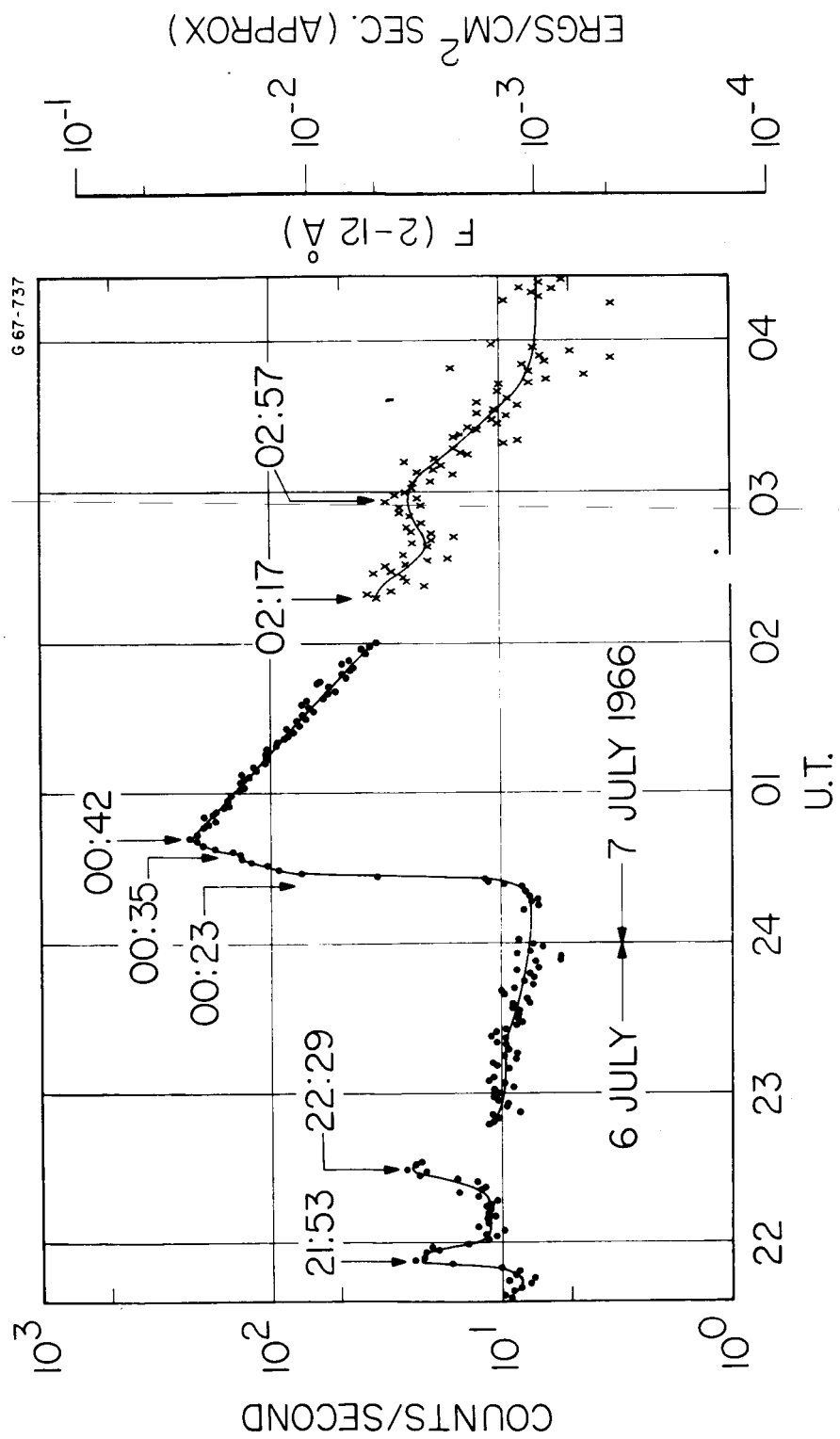


Figure 6

7 JULY 1966

G 67-733

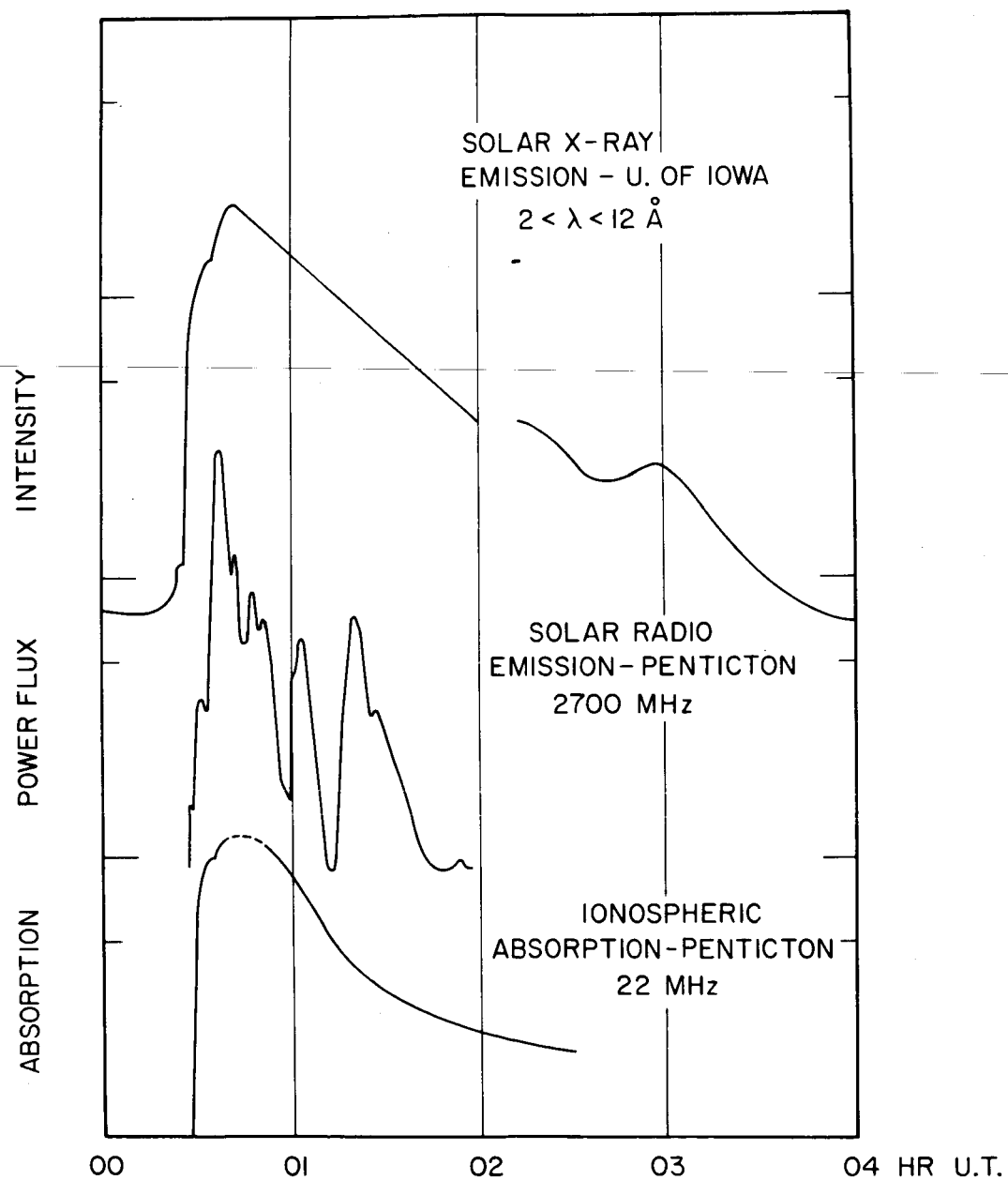


Figure 7

UNCLASSIFIED

Security Classification

DOCUMENT CONTROL DATA - R&D

(Security classification of title, body of abstract and indexing annotation must be entered when the overall report is classified)

1. ORIGINATING ACTIVITY (Corporate author)

University of Iowa
Department of Physics and Astronomy

2a. REPORT SECURITY CLASSIFICATION

UNCLASSIFIED

2b. GROUP

3. REPORT TITLE

The Solar X-Ray Flare of 7 July 1966

4. DESCRIPTIVE NOTES (Type of report and inclusive dates)

Progress July 1967

5. AUTHOR(S) (Last name, first name, initial)

Van Allen, J. A.

6. REPORT DATE

July 1967

7a. TOTAL NO. OF PAGES

31

7b. NO. OF REFS

9

8a. CONTRACT OR GRANT NO.

Nonr 1509(06)

9a. ORIGINATOR'S REPORT NUMBER(S)

U. of Iowa 67-35

b. PROJECT NO.

c.

9b. OTHER REPORT NO(S) (Any other numbers that may be assigned this report)

d.

10. AVAILABILITY/LIMITATION NOTICES

Distribution of this document is unlimited.

11. SUPPLEMENTARY NOTES

12. SPONSORING MILITARY ACTIVITY

Office of Naval Research

13. ABSTRACT

(See next page)